

THE ELODIE PLANET SEARCH: SYNTHETIC VIEW OF THE SURVEY AND ITS GLOBAL DETECTION THRESHOLD

D. Naef^{1,2}, M. Mayor², J.-L. Beuzit³, C. Perrier³, D. Queloz², J.-P. Sivan⁴, and S. Udry²

¹European Southern Observatory, Alonso de Cordova 3107, Santiago 19, Chile

²Observatoire de Genève, 51 ch. des Maillettes, CH-1290 Sauverny, Switzerland

³Laboratoire d'Astrophysique de Grenoble, UJF, BP 53, F-38041 Grenoble, France

⁴Laboratoire d'Astrophysique de Marseille, Traverse du Siphon, BP 8, F-13376 Marseille, France

ABSTRACT

In this paper, we give a synthetic view of the ELODIE Planet Search programme: a short description of our instrument and the surveyed sample as well as a brief review of our detections. Moreover, we have obtained, through numerical simulations, the global survey sensitivity: a detection probability map in the m_2 versus P diagram. We use this map for correcting our total number of detections for observational biases. Finally we derive the fraction of our sample stars hosting at least one giant planet.

Key words: Planets: exoplanets – Techniques: radial velocities

Table 1. The 18 objects with minimum masses below 18 M_{Jup} detected with ELODIE and planet candidates confirmed with this instrument

Planet	Reference
51 Peg b	Mayor & Queloz 1995
14 Her b	Naef et al. 2004
Gl 876 b	Delfosse et al. 1998
HD 209458 b	Mazeh et al. 2000
HD 190228 b	Perrier et al. 2003
HD 8574 b	Perrier et al. 2003
HD 50554 b	Perrier et al. 2003
HD 74156 b	Naef et al. 2003
HD 74156 c	Naef et al. 2003
HD 80606 b	Naef et al. 2001
HD 106252 b	Perrier et al. 2003
HD 178911 Bb	Zucker et al. 2002
HD 20367 b	Udry et al. 2002
HD 23596 b	Perrier et al. 2003
HD 33636 b	Perrier et al. 2003
HD 37124 c	Udry et al. 2002
HD 150706 b	Udry et al. 2002
Gl 777 Ab	Naef et al. 2003
Confirmations	
Urs And b	Naef et al. 2004
Urs And c	Naef et al. 2004
Urs And d	Naef et al. 2004
55 Cnc b	Naef et al. 2004
55 Cnc d	Naef et al. 2004
47 UMa b	Naef et al. 2004
70 Vir b	Naef et al. 2004
HD 187123 b	Naef et al. 2004

1. THE ELODIE SURVEY: QUICK VIEW

The search for extra-solar planets with the ELODIE echelle spectrograph (Baranne et al. 1996) mounted on the 193-cm telescope at Observatoire de Haute-Provence (OHP) started in 1994. The initial sample contained 142 stars, out of which 51 Peg (HD 217014), the star hosting the first detected extra-solar planet (Mayor & Queloz 1995). The sample was largely modified in 1997. The to-date survey sample size amounts to 330 stars. 18 extra-solar planet candidates have been detected with ELODIE. 15 of these candidates are orbiting a star in our sample. The three other detections (Gl 876 b, HD 80606 b and HD 178911 Bb) result from other programmes. Here are the main characteristics of our survey:

- **ELODIE:** $\frac{R}{\Delta R} = 42\,000$ echelle spectrograph mounted on the 193-cm telescope at OHP (CNRS, France). A detailed description of the instrument can be found in Baranne et al. 1996.
- **Instrumental precision:** $\simeq 6.5 \text{ m s}^{-1}$ (see Perrier et al. 2003).
- **Sample:** 330 solar-type stars brighter than $m_V=7.65$ in the northern hemisphere. The fast rotators ($v \sin i > 4 \text{ km s}^{-1}$) and the binaries were removed according to CORAVEL (Baranne et al. 1979) radial-velocity data (see Perrier et al. 2003 for details).
- **Detections:** 18 planets detected (15 within the above described planet-search sample). Some of these planets are in multiple systems: HD 37124 c (Udry et al. 2002); HD 74156 b and c (Naef et al. 2004). The complete list of the to-date ELODIE detections and the corresponding references are presented in table 1. As an example of detection, Fig. 1 shows the ELODIE updated orbital solution for 51 Peg published in Naef et al. 2004.
- **Confirmations:** Using ELODIE, we have confirmed the orbital solution for planet candidates around Urs And (HD 9826, Butler et al. 1997, Butler et al. 1999) 55 Cnc (HD 75732, Butler et al. 1997, Marcy et al. 2002), 47 UMa (HD 95128, Butler & Marcy 1996), 70 Vir (HD

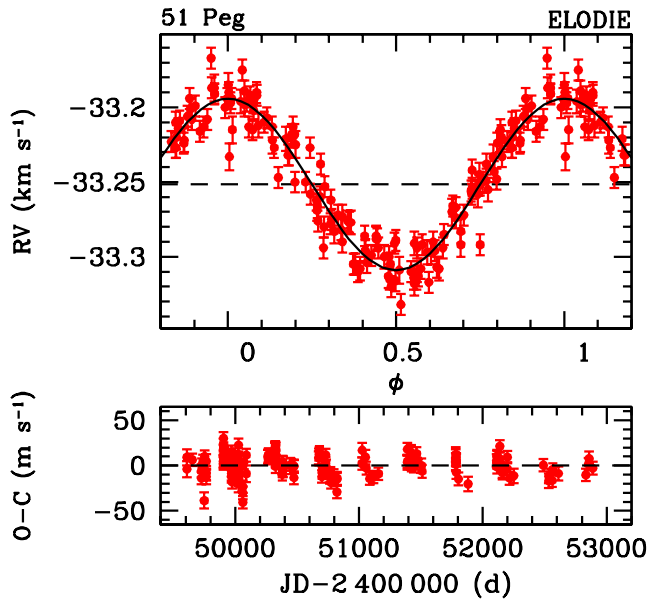


Figure 1. 3000 days of 51 Peg radial-velocity follow-up. Top: phase-folded ELODIE velocities and fitted orbital solution. Bottom: residuals to the fitted orbit. Figure from Naef et al. 2004.

117176, Marcy & Butler 1996) and HD 187123 (Butler et al. 1998). These confirmed planetary companions are also listed in table 1.

2. GLOBAL ELODIE SURVEY SENSITIVITY

We have determined, via numerical simulations, the global ELODIE survey sensitivity, i.e. the probability of detection in the secondary mass versus orbital period diagram. We give some details about these simulations in Sect. 2.1. In Sect. 2.2, we describe how we accounted for non-photon error sources. We study the impact of various stellar properties on the sensitivity in Sect. 2.3. Finally, we present our results in Sect. 2.4.

2.1. NUMERICAL SIMULATIONS

We have computed, through numerical simulations, the detection probabilities for a grid in the m_2 versus P diagram. The secondary mass and orbital period considered intervals are: $0.025 \leq m_2 \leq 20 M_{\text{Jup}}$ and $0.8 \leq P \leq 6000$ d. The total number of grid points is 3534. We have generated 5000 random orbits for each grid point using the following distributions:

- uniform distribution for T_0 (instant of periastron passage) and ω (longitude of the periastron)
- e (orbital eccentricity): we have used the eccentricity distribution observed for the known extra-solar planet candidates
- i (inclination of the orbital plane): the probability density we have used for i is proportional to $\sin i di$

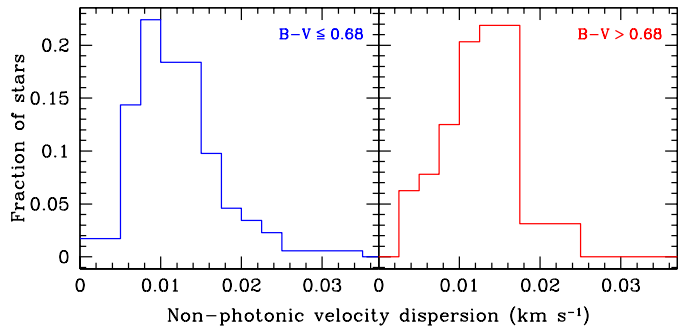


Figure 2. Distributions of non-photon error sources obtained for the ELODIE planet search sample. Two colour intervals have been considered: $B - V \leq 0.68$ (left) and $B - V > 0.68$ (right). We see that the non-photon noise only weakly depends on star colours.

Our simulation algorithm accounts for:

- the stellar content of our sample (i.e. the M_1 , m_V , $B - V$, $[\text{Fe}/\text{H}]$ and $v \sin i$ distributions for our sample)
- the real timing of the radial-velocity observations
- weather and seeing conditions at OHP
- the presence of non-photon error sources such as stellar activity jitter (see Sect 2.2)

2.2. NON-PHOTONIC ERROR SOURCES

In order to account for the presence of non-photon velocity error sources, we have determined the distribution of the observed velocity dispersion corrected for the photon noise for a subsample of target stars. This subsample contains the non-variable stars and the micro-variable stars for which the variability origin is unknown. The stars with planetary companions, the spectroscopic binaries (SB1 or SB2), the stars with close visual companions and the stars with blended spectra have been removed.

Figure 2 shows the distributions of the velocity dispersion for the remaining targets (240 stars). Their velocity dispersions have been quadratically corrected for their mean photon noise for building the displayed distributions. The remaining velocity dispersion sources present in these distributions are: the instrumental error, the stellar jitter, the stellar oscillations, the non-detected (or not yet characterized) light planets and the non-detected blended spectra. Non-photon error contributions have been randomly generated in our simulations using these two distributions.

2.3. IMPACT OF COLOUR, METALLICITY AND ROTATION

Figure 3 shows the impact of the $B - V$ colour index, the metallicity $[\text{Fe}/\text{H}]$ and the projected rotational velocity $v \sin i$ on the 90% detection limit obtained using the measurement dates and signal-to-noise ratios obtained for one of our sample stars. The photon noise errors have been

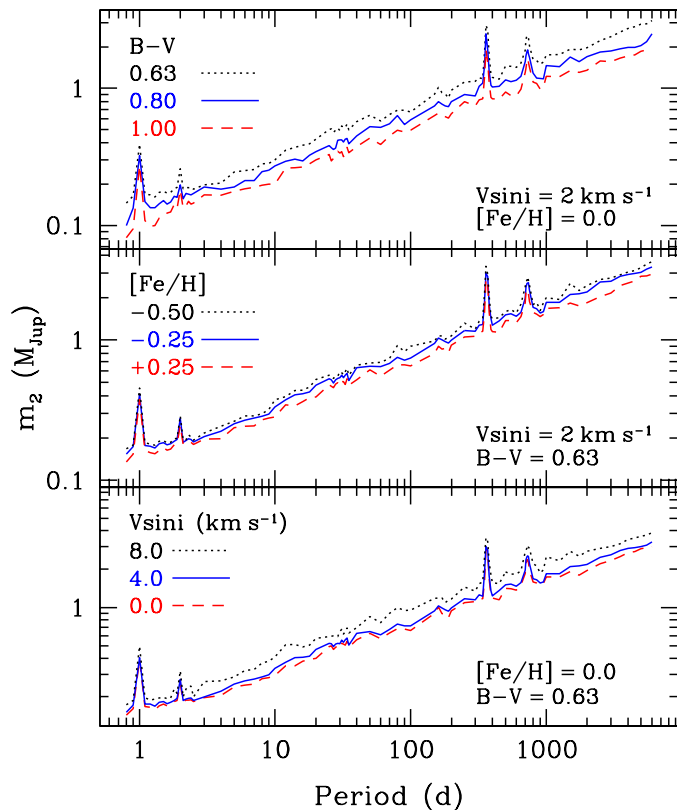


Figure 3. Impact of stellar properties on the 90% detection limit of one sample star: $B - V$ (top), $[Fe/H]$ (middle) and $v \sin i$ (bottom). An almost negligible impact of rotation and a weak impact of metallicity are observed. The moderate impact of colour is mostly due to the differences in primary mass.

computed using cross-correlation function parameters corresponding to the simulated stellar characteristics.

The impact of rotation is negligible up to $v \sin i = 4 \text{ km s}^{-1}$, the value we have used for selecting our sample of slow rotators. The impact of metallicity is very weak whereas the impact of colour is higher but mostly due to primary mass differences. The absence of metallicity impact on the detection limits further demonstrates that the observed difference between the metallicity distributions for stars with and without planets (Santos et al. 2001, Santos et al. 2004) does not result from an observational bias.

2.4. RESULTS

Figure 4 shows the 50 and 90% typical detection limits for the ELODIE survey. The dotted curve is the 90% detection limit we would obtain without the presence of any non-photonic error source but the instrumental error (here set to 6.5 m s^{-1}). The filled dots are the planet detected around stars in our sample. Open triangles are used for planets detected with ELODIE outside our sample and for

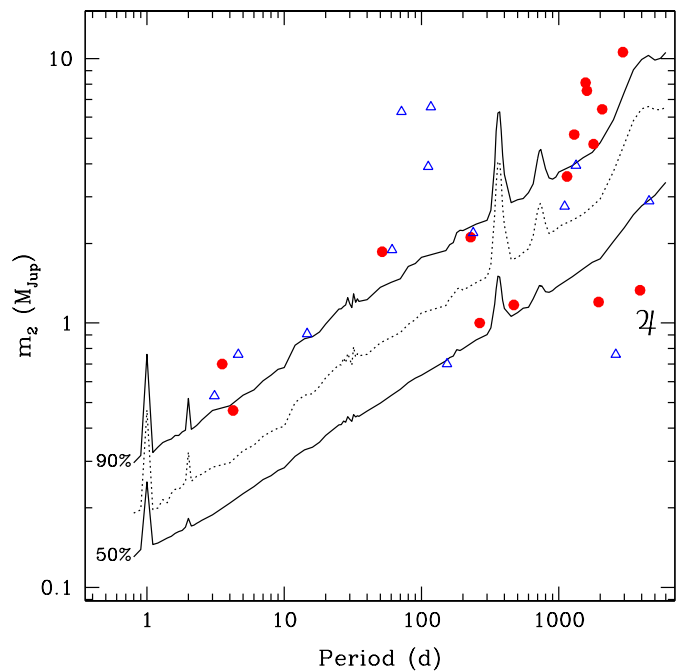


Figure 4. ELODIE 50 and 90% global detection limits (solid lines). The dotted curve is the 90% detection limit obtained without including non-photonic error sources except the 6.5 m s^{-1} instrumental error. This illustrates the dramatic impact of these error sources (in particular the radial-velocity jitter induced by stellar activity). Planets detected around our sample stars are noted by filled dots. The open triangles represent planet detected with ELODIE around stars outside our sample or detections confirmed with ELODIE. The position of Jupiter is indicated with its symbol.

planets confirmed with ELODIE. The main trend of these curves is proportional to $P^{1/3}$ as expected from Kepler's laws. We note the enormous sensitivity decrease at $P=1$ and 2 days and 1 and 2 years.

Probabilities of detection versus orbital period for different secondary masses ($1 M_{\text{Sat}}$, $1 M_{\text{Jup}}$ and $10 M_{\text{Jup}}$) are displayed in Fig. 5. The presence of non-photonic error sources is taken into account. 90% of the Jupiter-mass planets are detected up to $P \simeq 20 \text{ d}$ and 50% up to $P = 300 \text{ d}$. The probability of detection for brown-dwarf companions is above 90% for all the period interval. The daily and yearly features are also clearly visible here. The dotted curves are obtained without including the contribution of non-photonic error sources except for the 6.5 m s^{-1} instrumental error. These curves clearly show the dramatic impact of stellar jitter (and other error sources) on the detection sensitivity.

We find no sensitivity decrease between 1 and 2 days. Thus, planets in this period range, the so-called "very hot Jupiters" (see e.g. Konacki et al. 2003, Bouchy et al. 2004,

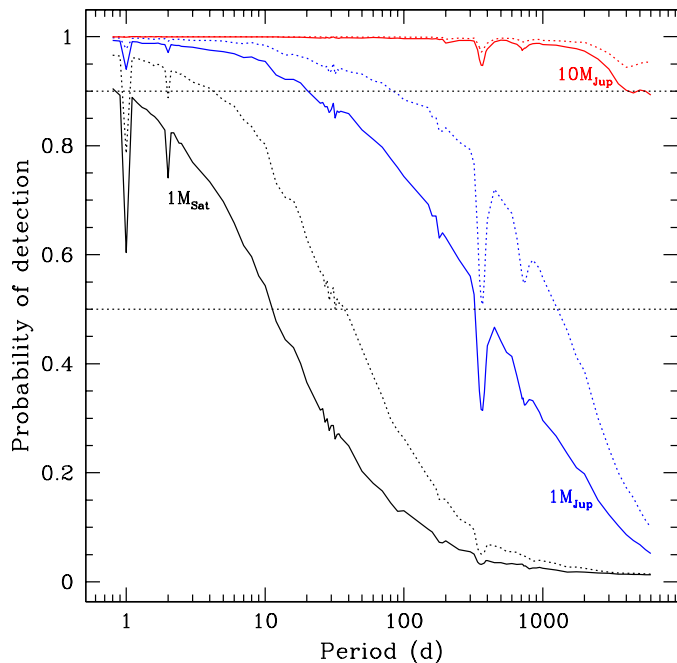


Figure 5. ELODIE detection probability versus orbital period for various companion masses (solid curves). The dotted curves represent the detection probabilities obtained without accounting for non-photonic error sources.

Konacki et al. 2004), would be easily detected if present around our sample stars.

3. FRACTION OF STARS HOSTING A GIANT PLANET

Following our obtained ELODIE detection limits, we can correct our effective detections for all the observational biases. We can also derive, by inverting the detection probability map, the fraction f of stars in our sample hosting at least one giant planet (the outer planets of the two systems are not considered here) with $m_2 \geq 0.47 M_{\text{Jup}}$ and for different period intervals. We find:

$$\begin{aligned}
 f &= 0.7 \pm 0.5\% \text{ for } P < 5 \text{ d} \\
 f &= 4.0 \pm 1.1\% \text{ for } P < 1500 \text{ d} \\
 f &= 7.3 \pm 1.5\% \text{ for } P < 3900 \text{ d}
 \end{aligned}$$

Details about our numerical simulations and these results on the global ELODIE survey sensitivity will be published in a forthcoming paper (Naef et al. 2004 in prep.).

ACKNOWLEDGEMENTS

We acknowledge support from the Swiss National Research Found (FNS), the Geneva University and the French CNRS. We are grateful to the Observatoire de Haute-Provence for the

generous time allocation and for the constant support during the last ten years.

REFERENCES

- Baranne A., Mayor M., Poncet J.L., 1979, *Vistas in Astron.* 23, 279
 Baranne A., Queloz D., Mayor M. et al., 1996, *A&AS* 119, 373
 Butler R.P., Marcy G.W., 1996, *ApJ* 464, L153
 Butler R.P., Marcy G.W., Williams E. et al., 1996, *ApJ* 474, L115
 Butler R.P., Marcy G.W., Vogt S.S. et al., 1998, *PASP* 110, 1389
 Butler R.P., Marcy G.W., Fischer D.A. et al., 1996, *ApJ* 526, 916
 Bouchy F., Pont F., Santos N.C. et al., 2004, *A&A* 421, L13
 Delfosse X., Forveille T., Mayor M. et al., 1998, *A&A* 338, L68
 Konacki M., Torres G., Jha S. et al., 2003, *Nature* 421, 507
 Konacki M., Torres G., Sasselov D. et al., 2004, *ApJ* 609, 137
 Mayor M., Queloz D., 1995, *Nature* 378, 355
 Marcy G.W., Butler R.P., 1996, *ApJ* 464, L147
 Marcy G.W., Butler R.P., Fischer D.A., et al., 2002, *ApJ* 581, 1375
 Mazeh T., Naef D., Torres G. et al., 2000, *ApJ* 532, L55
 Naef D., 2003, PhD Thesis, Geneva Observatory
 Naef D., Latham D., Mayor M. et al., 2001, *A&A* 375, L27
 Naef D., Mayor M., Korzennik S. et al., 2003, *A&A* 410, 1051
 Naef D., Mayor M., Beuzit J.L. et al., 2004, *A&A* 414, 351
 Perrier C., Sivan J.P., Naef D. et al., 2003, *A&A* 410, 1039
 Santos N.C., Israelian G., Mayor M., 2001, *Nature* 411, 163
 Santos N.C., Israelian G., Mayor M. et al., 2003, *A&A* 398, 363
 Santos N.C., Israelian G., Mayor M., 2004, *A&A* 415, 1153
 Udry S., Mayor M., Queloz D., 2003, in "Scientific Frontiers in Research on Extrasolar Planets"
 Zucker S., Naef D., Latham D.W. et al., 2002, *ApJ* 568, 363